RESEARCH ARTICLE

Analysis of LCL Filter Topologies for DC-DC Isolated Cuk Converter at CCM Operation

ERDAL ŞEHIRLI[ID]
Department of Electrical and Electronics Engineering, Kastamonu University, 37150 Kastamonu, Turkey

e-mail: esehirli@kastamonu.edu.tr

ABSTRACT In this study, the application and analysis of LCL filter topologies including an LCL, an LCL with damping, and an LCL trap filter used by a DC-DC isolated Ćuk converter operated at CCM are presented. The converter is designed for 50 W with 42 kHz switching frequency using a SiC MOSFET as a power switch. Although LCL filter topologies are commonly used with an inverter, their use in DC-DC converters has not been studied in detail. The main contribution of the paper is the application, design, and analysis of an LCL trap filter, which is not presented for a DC-DC converter in the literature, as an input filter of a DC-DC isolated Ćuk converter. For exact analysis of the effect of the filter, as a second main contribution of the paper, a state-space average mathematical model, small signal analysis of an isolated Ćuk converter for CCM operation, which was not presented before in the literature, is derived and its transfer function is obtained. In this paper, the practical design and transfer functions of LCL-based filter topologies are also presented. In order to analyze the effect of filter topologies by using linear methods including root locus and Bode graphs, the transfer function of the converter is cascaded with the transfer function of each filter separately, which is the third contribution of the paper because such analysis has not been presented in the literature. Furthermore, each cascaded transfer function and the transfer function of the converter are validated by step responses. All LCL filters, with an LC filter for comparison, are employed in the experimental setup. Owing to the applications, control characteristics and input current ripples are measured. In addition, the efficiencies of each different structure are determined. As a result of the analysis and measurements, the LCL trap filter gives better results in terms of efficiency (86%) and input current ripple (0.96 A peak). Moreover, the LCL with damping filter gives poorer control characteristics, but the maximum gain of the controller avoiding the instability of LCL with damping is 0.0855, which is higher than that of the others. Furthermore, it is shown that each LCL filter topology provides a 45% lower total inductor value compared to the LC filter.

INDEX TERMS CCM, isolated Cuk, LCL, LC, small-signal, trap.

I. INTRODUCTION

Filter design is one of the most crucial points for power converters. Mainly, the purpose of the filter is to reduce the high frequency noise of the power switch and minimize current ripples. In addition, for DC-DC converters, the traditional LC filter is the most preferred structure. However, by comparing LCL-based filters, which are not studied in the literature in detail for DC-DC converters, the LC filter has a higher total inductor value. Therefore, the use of an LCL

filter makes the use of a lower total inductor value possible. In addition, to obtain galvanic isolation by using a high frequency transformer on the power converter is very important because of providing electrical isolation and adjusting lower output voltage values. Hence, the use of a DC-DC isolated Ćuk converter is very eye-catching due to its high frequency transformer and inductors at both the input and outside of the converter reducing current ripple.

In the literature, filter design and an isolated Ćuk converter are introduced in some studies as given below.

The review and design considerations of passive filters, mainly LCL-based type topologies, are introduced for three

The associate editor coordinating the review of this manuscript and approving it for publication was Norbert Herencsar[ID].

phase converters in [1]. The design and analysis of an LCL with damping filter is presented for inverter application in [2] and for a three phase PWM rectifier in [3] without considering the cascaded transfer function. For a single phase PFC converter the design and application of the LC filter are given in [4] without modeling the filter. The design and application of an LCL trap filter for inverter applications are presented in [5], [6], [7], and [8]. Reference [9] proposes an LCL trap filter for a three phase PWM rectifier without considering the effect of the converter by simulation study. The fundamental analysis, design, and theory of an isolated Cuk converter without deriving state-space model is presented in [10], [11], and [12]. Circuit-based small signal analysis of a DC-DC isolated Cuk converter considering the magnetization effect without a state-space model and application for DCM operation is given in [13]. Designing by reduced transfer function using a circuit-based model of a three stage isolated Cuk converter for DCM operation is given in [14]. Reference [15] and [16] present an isolated PFC Cuk converter as a LED driver application without using its model and giving information about the input filter. An isolated PFC Cuk converter using an LC filter without considering its effect on the converter is presented with a bridgeless type in [17] and with a bridge rectifier in [18] as a front-end converter for motor drive application. Reference [19] and [20] present a PFC isolated Cuk converter without deriving a state-space model and small signal analysis for battery charging applications.

In addition, to the references stated above, filter designs including LC, LCL, LCL with damping, and LCL trap filters with respect to power converters in the literature are summarized in Table 1. The converters in the table are classified as DC-DC, DC-AC, and AC-DC. It can be seen from the table that an LCL trap filter is not presented for DC-DC converters in the literature. Moreover, LCL in [25], [26], and [27] and LCL with damping filter in [32] and [33] for DC-DC converters are simulation-based studies and there are no application results showing the effect of LCL type filters for DC-DC converters.

TABLE 1. Filter design by topologies with respect to converter types in literature.

Converter	LC	LCL	LCL with damping	LCL trap
DC-DC	[21], [22]	[25], [26], [27]	[32], [33]	-
DC-AC	[23]	[28], [29]	[2], [34]	[5], [6], [7], [8]
AC-DC	[4], [24]	[30], [31]	[3], [35]	[9], [36]

Furthermore, in the literature a comparison of the filter types is presented. However, the studies are conducted by simulations. For instance, [37] includes a comparison of L, LC, and LCL filters for a distribution system without application, just a simulation study, and it concludes that the LCL filter gives higher attenuation and lower total inductor values. Reference [38] compares LC, LCL, and LCL with damping

resistor by simulation study for a single phase inverter and it shows that the LCL with damping filter provides optimum efficiency. L and LCL with damping filters are compared in [39] and [40] with a three phase PWM rectifier by simulation and [39] shows that the L filter gives better performance with respect to THD and efficiency, while [40] states that the LCL filter provides lower total inductance and higher power loss on the damping resistor. Reference [41] and [42] compare L, LC, and LCL filters in a simulation study for inverter applications and it is concluded that the LCL filter provides better attenuation with lower inductance. Comparison of LCL and LCL trap filters is realized by simulation study for a three phase rectifier in [43] and for a three phase inverter in [44] and [43] concludes that LCL trap filter topology provides less harmonic distortion and [44] states that both filters ensure the limits.

In addition, comparisons of different filter design methodologies using common and differential mode noises with different combinations of LC filter for DC-DC converter and electrical motor without considering the control effect of the converter and electrical motor are presented in [45] and [46]. Reference [47] designs a magnetic integrated LCL filter for a single phase inverter with a SiC MOSFET and it shows that the volume and weight of the filter are less than those of a traditional LCL filter.

Moreover, some studies in the literature analyze the filter effect and its stability. For example, the effect of an LC filter on a DC-DC buck and boost converter by using Bode plots with small signal analysis and cascading the filter transfer function without applications in [48] and [49] and with application for a DC-DC boost converter in [50] is examined. Reference [51] analyzes the LC filter's effect on a DC-DC buck-boost converter by cascading converter and filter transfer function without application. Stability analysis of LC-based filters with different damping structures is realized in [52] for DC-DC converters without considering the converter transfer function. Stability analysis and active stabilization for constant power loads are presented by using an LC filter with a DC-DC buck converter in [53] and [54] and for a boost converter in [55] and [56] presents Lyapunov-based control of a DC-DC boost converter using an LC filter by integrating a filter mathematical model. Reference[57] presents stability analysis of a multi-trap LCL filter by using a grid connected converter without considering the transfer function of the converter. State-space control of an inverter using an LCL filter is presented in [58]. Reference [59] presents state-space control of a three phase PWM converter using an LCL filter considering the filter effect and it is concluded that the LCL filter-based system gives better performance than the L filter-based system.

After the literature review, it can be concluded that different input filter types used for the DC-DC converter are not analyzed deeply using small signal models and cascaded transfer functions with respect to control characteristic and input ripple reduction. Therefore, the present paper presents the analysis, application, and comparison of the LCL type

input filter topologies including LCL, LCL with damping, and LCL trap filters with a DC-DC isolated Ćuk converter designed for 50 W power with 42 kHz switching frequency using a SiC power switch. In the literature an LCL type filter especially an LCL trap filter is not presented for a DC-DC converter. One of the main unique contributions of the paper is the design, analyses, and implementation of an LCL trap filter as an input filter of a DC-DC isolated Ćuk converter. After the applications, comparisons are made with respect to input current, efficiency, and control. Further, to make a general comparison an LC type filter is included. As a second unique contribution of the paper, the state-space average model of the DC-DC isolated Ćuk converter operated in CCM is derived, small signal analysis is performed, and the transfer function is obtained, and the transfer function is analyzed by linear methods including root locus and Bode graphs. In addition, the transfer function and practical design of each filter topology is obtained and cascaded transfer functions of each filter with the transfer function of the DC-DC isolated Ćuk converter are derived. Then the effects of each filter topology on the transfer functions are analyzed by linear methods for the control point of view as such analysis has not been introduced in the literature before. Due to the applications, the effects of each filter on efficiency, input current ripple, and control characteristics are compared. As a result, the LCL trap filter is better than the others by giving 86% efficiency and 0.96 A current ripple. Moreover, for the control point of view each filter has similar characteristics but LCL with damping gives a poorer result. Furthermore, the total inductor value with the LCL based filters is reduced 45% compared with the LC filter.

II. MODELING OF ISOLATED CUK DC-DC CONVERTER

In Fig. 1 the circuit structure of a DC-DC isolated Ćuk converter having a diode bridge, a high frequency transformer, two capacitors and two inductors, a power diode, and a power switch is shown.
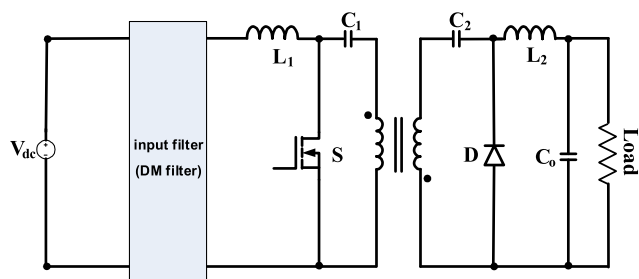

FIGURE 1. Circuit structure of isolated Ćuk DC-DC converter.

The operating principle of the DC-DC isolated Ćuk converter is explained by the switch's on and off positions. When the power switch is on, L_1 stores energy and C_1 charges C_2 by the power switch, diode, and high frequency transformer. Moreover, L_2 transfers its energy to the load by power diode. When the power switch is off, C_1 is charged by L_1 and input source and C_2 discharges to L_2 and to load.

The passive components of the converter can be calculated using (1), (2), (3), (4), (5). For CCM mode of operation inductor values should be higher than the calculated values in (1), (2).

$$L_1 = \frac{R_L(1-D)^2}{2Df_s n^2} = \frac{12.5 \times (1-0.47)^2}{2 \times 0.47 \times 42000 \times 0.2^2} = 2.2 \text{ mH} \tag{1}$$

$$L_2 = \frac{R_L(1-D)}{2f_s} = \frac{12.5 \times (1-0.47)}{2 \times 42000} = 78.9 \mu H \tag{2}$$

$$C_1 = \frac{V_{in}n^2 D^2}{(1-D)\Delta V_{C1}f_s R_L}$$
$$= \frac{142 \times 0.2^2 \times 0.47^2}{(1-0.47) \times 10 \times 42000 \times 12.5} = 451 \text{ nF} \tag{3}$$

$$C_2 = \frac{V_o D}{\Delta V_{C2}f_s R_L} = \frac{25 \times 0.47}{24 \times 42000 \times 12.5} = 933 \text{ nF} \tag{4}$$

$$C_o \geq \frac{V_o(1-D)}{8L_2\Delta V_{Co}f_s^2}$$
$$= \frac{25 \times (1-0.47)}{8 \times 654 \times 10^{-6} \times 10 \times 42000^2} = 143 \text{ nF} \tag{5}$$

The state-space average mathematical model of the DC-DC isolated Ćuk converter for CCM operation of the input inductor can be derived with regard to the switch's on and off position as shown in Fig. 2.
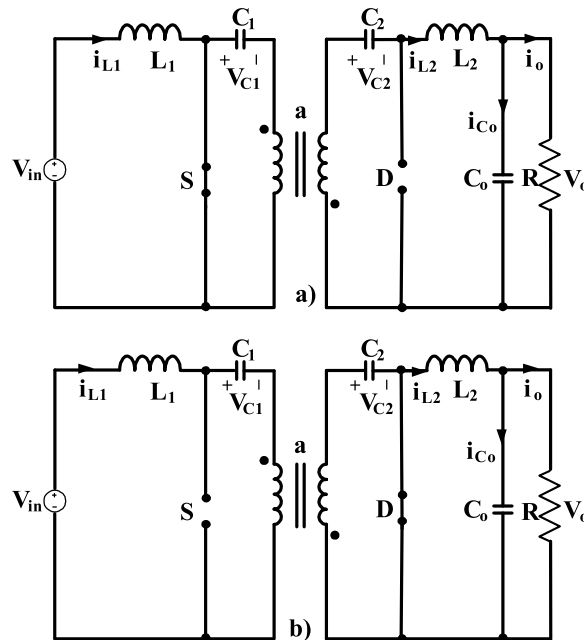

FIGURE 2. Isolated Ćuk DC-DC converter, a) switch on and b) switch off circuits.

In order to derive the state-space mathematical model of the converter, Kirchhoff's voltage and current laws are applied to the switch's on and off circuits separately.

The model can be derived for the switch on position in (6), (7), (8), (9), (10), (11).

$$\frac{di_{L1}}{dt} = \frac{V_{in}}{L_1} \tag{6}$$

$$\frac{dV_{C1}}{dt} = \frac{-ai_{L2}}{C_1} \tag{7}$$

$$\frac{di_{L2}}{dt} = \frac{V_{C1}}{aL_2} + \frac{V_{C2}}{L_2} - \frac{V_o}{L_2} \tag{8}$$

$$\frac{dV_{C2}}{dt} = \frac{i_{L2}}{C_2} \tag{9}$$

$$\frac{dV_o}{dt} = \frac{i_{L2}}{C_0} - \frac{V_0}{RC_0} \tag{10}$$

$$\begin{bmatrix} \dot{i}_{L1} \\ V_{C1} \\ i_{L2} \\ V_{C2} \\ V_o \end{bmatrix} = \begin{bmatrix} 0 & 0 & 0 & 0 & 0 \\ 0 & 0 & \frac{-a}{C_1} & 0 & 0 \\ 0 & \frac{1}{aL_2} & 0 & \frac{1}{L_2} & \frac{-1}{L_2} \\ 0 & 0 & \frac{1}{C_2} & 0 & 0 \\ 0 & 0 & \frac{1}{C_0} & 0 & \frac{-1}{RC_0} \end{bmatrix} \begin{bmatrix} i_{L1} \\ V_{C1} \\ i_{L2} \\ V_{C2} \\ V_o \end{bmatrix} + \begin{bmatrix} \frac{1}{L_1} \\ 0 \\ 0 \\ 0 \\ 0 \end{bmatrix} V_{in} \tag{11}$$

For the switch off position, the model can be written in (12), (13), (14), (15), (16), (17).

$$\frac{di_{L1}}{dt} = \frac{-V_{C1}}{L_1} - \frac{aV_{C2}}{L_1} + \frac{V_{in}}{L_1} \tag{12}$$

$$\frac{dV_{C1}}{dt} = \frac{i_{L1}}{C_1} \tag{13}$$

$$\frac{di_{L2}}{dt} = \frac{-V_o}{L_2} \tag{14}$$

$$\frac{dV_{C2}}{dt} = \frac{ai_{L1}}{C_2} \tag{15}$$

$$\frac{dV_o}{dt} = \frac{i_{L2}}{C_0} - \frac{V_0}{RC_0} \tag{16}$$

$$\begin{bmatrix} \dot{i}_{L1} \\ V_{C1} \\ i_{L2} \\ V_{C2} \\ V_o \end{bmatrix} = \begin{bmatrix} 0 & \frac{-1}{L_1} & 0 & \frac{-a}{L_1} & 0 \\ \frac{1}{C_1} & 0 & 0 & 0 & 0 \\ 0 & 0 & 0 & 0 & \frac{-1}{L_2} \\ \frac{a}{C_2} & 0 & 0 & 0 & 0 \\ 0 & 0 & \frac{1}{C_0} & 0 & \frac{-1}{RC_0} \end{bmatrix} \begin{bmatrix} i_{L1} \\ V_{C1} \\ i_{L2} \\ V_{C2} \\ V_o \end{bmatrix} + \begin{bmatrix} \frac{1}{L_1} \\ 0 \\ 0 \\ 0 \\ 0 \end{bmatrix} V_{in} \tag{17}$$

To obtain the average state-space model of the converter given in (19), (11) and (17) are combined by the condition of (18).

$$A = dA_1 + (1-d)A_2, \ B = dB_1 + (1-d)B_2 \tag{18}$$

$$\begin{bmatrix} \dot{i}_{L1} \\ V_{C1} \\ i_{L2} \\ V_{C2} \\ V_o \end{bmatrix} = \begin{bmatrix} 0 & \frac{-(1-d)}{L_1} & 0 & \frac{-a(1-d)}{L_1} & 0 \\ \frac{1-d}{C_1} & 0 & \frac{-ad}{C_1} & 0 & 0 \\ 0 & \frac{d}{aL_2} & 0 & \frac{d}{L_2} & \frac{-1}{L_2} \\ \frac{a(1-d)}{C_2} & 0 & \frac{d}{C_2} & 0 & 0 \\ 0 & 0 & \frac{1}{C_0} & 0 & \frac{-1}{RC_0} \end{bmatrix}$$
$$\times \begin{bmatrix} i_{L1} \\ V_{C1} \\ i_{L2} \\ V_{C2} \\ V_o \end{bmatrix} + \begin{bmatrix} \frac{1}{L_1} \\ 0 \\ 0 \\ 0 \\ 0 \end{bmatrix} V_{in} \tag{19}$$

In order to derive the linear model and transfer function of the DC-DC isolated Ćuk converter, small signal analysis of the converter should be conducted. The small signal equivalent model can be obtained in (21) by using (20).

$$\dot{\tilde{x}} = (dA_1 + (1-d)A_2)\tilde{x} + [(A_1 - A_2)\tilde{x} + (B_1 - B_2)u]\tilde{d} \tag{20}$$

$$\begin{bmatrix} \dot{\tilde{i}}_{L1} \\ V_{C1} \\ i_{L2} \\ V_{C2} \\ V_o \end{bmatrix} = \begin{bmatrix} 0 & \frac{-(1-d)}{L_1} & 0 & \frac{-a(1-d)}{L_1} & 0 \\ \frac{1-d}{C_1} & 0 & \frac{-ad}{C_1} & 0 & 0 \\ 0 & \frac{d}{aL_2} & 0 & \frac{d}{L_2} & \frac{-1}{L_2} \\ \frac{a(1-d)}{C_2} & 0 & \frac{d}{C_2} & 0 & 0 \\ 0 & 0 & \frac{1}{C_0} & 0 & \frac{-1}{RC_0} \end{bmatrix}$$
$$\times \begin{bmatrix} \widetilde{i}_{L1} \\ V_{C1} \\ i_{L2} \\ V_{C2} \\ V_o \end{bmatrix} + \begin{bmatrix} \frac{V_{C1}+aV_{C2}}{L_1} \\ \frac{-i_{L1}-ai_{L2}}{C_1} \\ \frac{V_{C1}+aV_{C2}}{aL_2} \\ \frac{-ai_{L1}+i_{L2}}{C_2} \\ 0 \end{bmatrix} \tilde{d} \tag{21}$$

It is required to find the transfer function of the DC-DC isolated Ćuk converter to apply linear analysis such as root locus and Bode diagrams. In addition, the transfer function of (21) should be cascaded with each filter topology to achieve exact analysis. Thus, the transfer function of (21) is derived in (23) by using (22).

$$T(s) = \frac{\widetilde{V}_o}{\tilde{d}} = C(sI - A)^{-1}B \tag{22}$$

$$T(s) = \frac{\begin{matrix} s^3(\frac{V_{in} - \frac{V_{in}d}{d-1}}{C_0L_2a}) + s^2(\frac{d(\frac{V_{in}d^2}{R(d-1)^2} - \frac{V_{in}d}{Ra(d-1)})}{C_0L_2C_2} + \\ \frac{d(\frac{-V_{in}d^2}{Ra(d-1)^2} + \frac{V_{in}d}{R(d-1)})}{C_0L_2C_1a}) + s(\frac{(d-1)^2(V_{in} - \frac{V_{in}d}{d-1})}{C_0L_2C_1L_1a} \\ -\frac{-da(d-1)(V_{in} - \frac{V_{in}d}{d-1})}{C_0L_2C_2L_1} + \frac{(d-1)^2a(V_{in} - \frac{V_{in}d}{d-1})}{C_0L_2C_2L_1} - \\ \frac{-d(d-1)(V_{in} - \frac{V_{in}d}{d-1})}{aC_0L_2C_1L_1}) \end{matrix}}{\begin{matrix} s^5 + \frac{s^4}{RC_0} + s^3(\frac{1}{C_0L_2} + \frac{d^2}{C_1L_2} - \frac{d^2}{C_2L_2} + \frac{(d-1)^2}{C_1L_1} \\ + \frac{a^2(d-1)^2}{C_2L_1}) + s^2(\frac{C_2d^2 - C_1d^2}{C_0C_1C_2L_2R} + \frac{(d-1)^2}{C_1C_0L_1R} \\ + \frac{(d-1)^2a^2}{C_2C_0L_1R}) + s(\frac{(d-1)^2a^2}{C_2C_0L_1L_2} + \frac{(d-1)^2}{C_2C_0L_1L_2}) \end{matrix}} \tag{23}$$

III. FILTER TOPOLOGIES
As an input filter of the DC-DC isolated Ćuk converter, in the present study LCL-based filter topologies are employed. Firstly, practical filter design methods are summarized, and transfer functions of the filters are derived. The LC filter that is used most in the literature for DC-DC converters is included to make exact comparisons of the LCL-based filter topologies, i.e., LCL, LCL with damping, and LCL trap.

A. LC FILTER
The LC filter's structure is shown in Fig. 3. It consists of a filter inductor and a capacitor.

In order to calculate filter components practically without using a line impedance stabilizer network (LISN), (24) can be used as in [4], [21], and [22]. It should be considered that filter
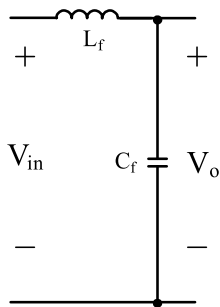
FIGURE 3. LC filter.

cut off frequency f_c should be much lower than switching frequency f_{sw}, practically 0.1 times lower.

$$L_f = \frac{1}{4\pi f_c^2 C_f}, \quad f_{sw} \gg f_c \tag{24}$$

The LC filter transfer function can be derived in (25).

$$T(s) = \frac{V_0}{V_{in}} = \frac{1}{s^2 L_f C_f + 1} \tag{25}$$

B. LCL FILTER WITH DAMPING

The LCL filter with a passive damping structure is shown in Fig. 4. It is popular to use an LCL filter with damping in inverter applications [2]. It can be also seen that a parallel capacitor is added at the output of the filter to increase the effectiveness of the LCL filter similar to as in [3].
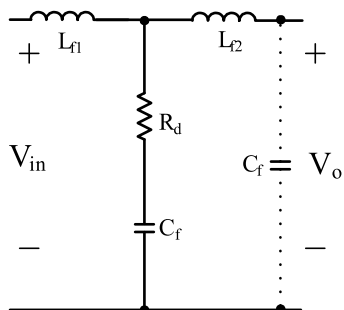
FIGURE 4. LCL filter with damping.

Damping resistance is calculated by using (26). The angular resonance frequency of the filter in (27) should meet the condition in (28). The relation of the filter inductors is given in (29), as in [2].

$$R_d = \frac{1}{3\omega_{res} C_f} \tag{26}$$

$$\omega_{res} = \sqrt{\frac{L_1 + L_2}{L_1 L_2 C_f}} \tag{27}$$

$$10 f_g < f_{res} < 0.5 f_{sw} \tag{28}$$

$$L_2 = r L_1 \tag{29}$$

The transfer function of the LCL filter with damping having parallel C_f is given in (30).

$$T(s) = \frac{V_0}{V_{in}} = \frac{R_d C_f L_2 s + L_2}{\begin{aligned}(s^4 C_f^2 L_{f2}^2 L_{f1} + s^3 (C_f^2 L_{f2}^2 R_d + \\ C_f^2 L_{f2} L_{f1} R_d) + s^2 (C_f L_{f2}^2 + 2 L_{f2} L_{f1} C_f) \\ + s L_{f2} R_d C_f + L_{f2})\end{aligned}} \tag{30}$$

C. LCL FILTER

The LCL filter structure is shown in Fig. 5. The filter does not have a damping resistor, which can increase power loss. The same equations (26), (27), (28), (29), (30) are used to calculate the passive components of the filter.
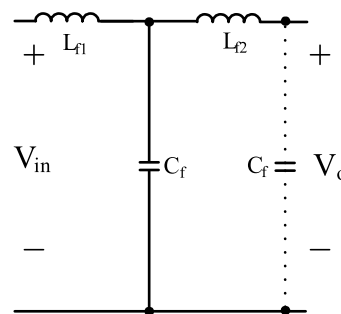

FIGURE 5. LCL filter.

The transfer function of the LCL filter is given in (31).

$$T(s) = \frac{V_0}{V_{in}} = \frac{L_2}{\begin{aligned}(s^4 C_f^2 L_{f2}^2 L_{f1} + s^2 (C_f L_{f2}^2 + L_{f2} L_{f1} C_f) + \\ s L_{f2} L_{f1} C_f^2 + L_{f2})\end{aligned}} \tag{31}$$

D. LCL TRAP FILTER

The LCL trap filter structure is shown in Fig. 6. It is seen that the filter has trap inductor L_T instead of R_d. In the literature, a trap LCL filter is used in inverter applications as in [5], [6], [7], and [8], but application of the filter for DC-DC converters is not presented in the literature.
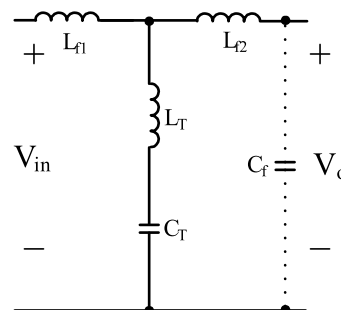

FIGURE 6. LCL trap filter.

Filter capacitor values C_f and C_T chosen can be the same as for the LC filter. The angular resonance frequency of the

filter is given in (32). The trap resonance frequency and the condition of the frequencies are given in (33), (34), as in [5], [6], [7], and [8].

$$\omega_{res} = \sqrt{\frac{L_1 + L_2}{C_T(L_1 L_2 + L_T L_2 + L_T L_1)}} \qquad (32)$$

$$f_T = \frac{1}{2\pi\sqrt{L_T C_T}} \qquad (33)$$

$$10 f_g < f_{res} < 0.5 f_T \qquad (34)$$

The transfer function of the LCL trap filter is given in (35).

$$T(s) = \frac{V_0}{V_{in}} = \frac{L_T C_T L_2 s^2 + L_2}{\begin{array}{c}(s^4 (C_f L_{f2}^2 L_T C_T + C_f L_{f2}^2 L_1 C_T) + \\ s^2 (C_f C_T L_{f2} L_{f1} L_T + C_f L_{f2}^2 + C_T L_{f2} L_T + \\ C_T L_{f2} L_{f1} + C_f L_{f2} L_{f1}) + L_{f2})\end{array}} \qquad (35)$$

IV. APPLICATIONS

Each filter type, including LC, LCL with damping, LCL, and LCL trap, are employed as an input filter of a DC-DC isolated Ćuk converter having 42 kHz switching frequency with 50 W power. Applications are conducted by using a GWInstek APS-9501 AC power supply, TPP0201 and P5122 voltage probes, A622 current probe, and TPS2024B oscilloscope. The laboratory setup is shown in Fig. 7. For the power switch a Cree C2M0280120D SiC MOSFET is used.

Passive values of the isolated DC-DC Ćuk converter are chosen as $L_1 = 5$ mH, $L_2 = 654$ μH, $C_1 = C_2 = 1$ μF, and $C_0 = 940$ μF after calculation with (1), (2), (3), (4), (5). The converter is designed for 50 W output power with 12.5 Ω load, and the turns ratio is 5. The input voltage is 130 V.

The transfer function of the converter in (23) is calculated as in (36) by using the passive values. It is vital to derive the transfer function of the converter in order to examine the effect of each filter structure by cascading them.

$$T(s) = \frac{\tilde{V}_o}{\tilde{d}} = \frac{8.66 \times 10^7 s^3 - 7.103 \times 10^{12} s^2 + 2.402 \times 10^{17} s}{\begin{array}{c}(s^5 + 85.11 s^4 + 1.462 \times 10^9 s^3 + \\ 1.243 \times 10^{11} s^2 + 2.376 \times 10^{15} s)\end{array}} \qquad (36)$$

By using the transfer function of the converter in (36), root locus and Bode graphs can be sketched as shown in Fig. 8. It is seen by the root locus that there are four poles at $3.55 \times 10^{-15} \pm 3.82 \times 10^4 j$, $-42.6 \pm 1.27 \times 10^3 j$ and two zeros at $4.07 \times 10^4 \pm 3.31 \times 10^4 j$. Zeros are in right half plane, making the system a nonminimum phase. By the Bode plot, gain margin is -35.1 dB and phase margin is $-23.6°$, meaning that the open loop DC-DC isolated Ćuk converter is unstable. Similar Bode plot responses of such a nonminimum phase system resulting in an unstable system are also obtained for Ćuk, boost, and SEPIC converters as in [60], [61], [62], and [63].

For filter applications, the passive values of each filter type are calculated by using (25), (26), (27), (28), (29),
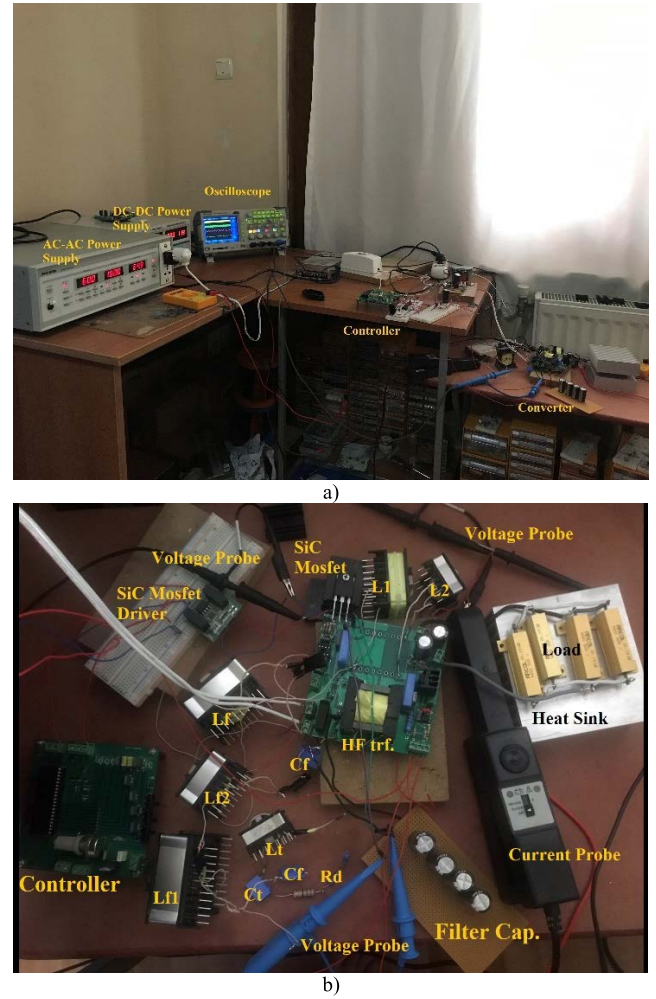

FIGURE 7. Laboratory setup, a) scope and sources, b) circuit.

(32), (33), (34) and they are given in Table 2. Although the filter inductor values are higher, lower inductor values can be obtained by changing filter capacitor value with higher values.

TABLE 2. Passive values used in paper.

Filter	L_f, (mH)	L_{f1}	L_{f2} (mH)	C_f (nF)	R_d (Ω)	L_T (μH)
LC	35	-	-	22	-	-
LCL with damping	9		10.2	22	155	-
LCL	9		10.2	-	-	-
LCL trap	9		10.2	22	-	652

A. LC FILTER

After cascading the transfer function of the LC filter given in (25) by using the passive value in Table 2, with the transfer function of the isolated Ćuk DC-DC converter in (36), the
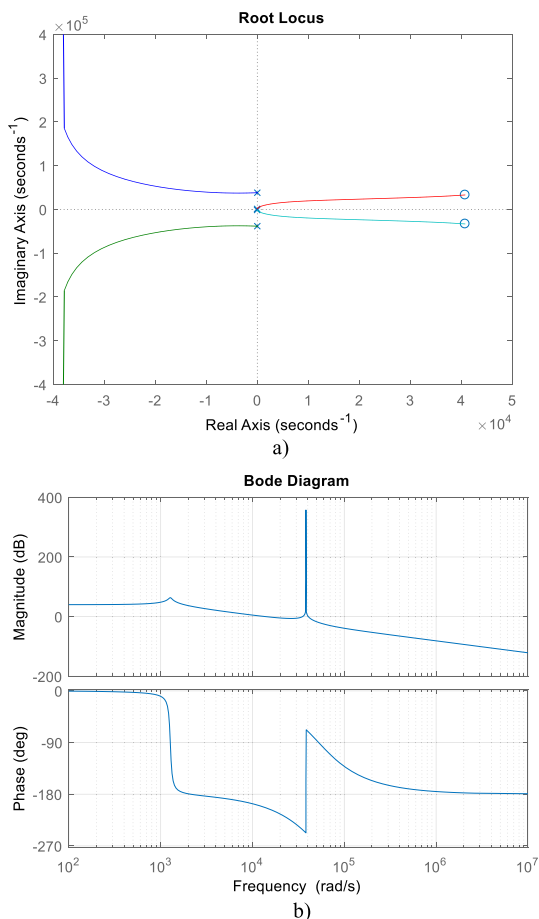
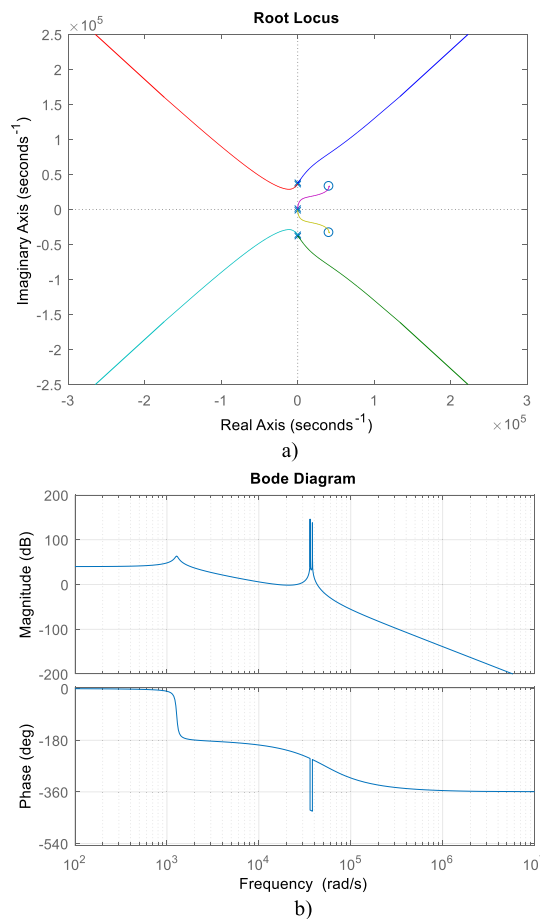**FIGURE 8.** a) Root locus, b) Bode graphs of isolated DC-DC Ćuk converter.

FIGURE 9. a) Root locus, b) Bode graphs of cascaded LC filter with converter.

cascaded transfer function is obtained in (37).

$$T(s) = \frac{\widetilde{V}_o}{\widetilde{d}} = \frac{\begin{pmatrix} 8.716 \times 10^7 s^3 - 7.103 \times 10^{12} s^2 + \\ 2.402 \times 10^{17} s \end{pmatrix}}{\begin{pmatrix} 7.7 \times 10^{-10} s^7 + 6.553 \times 10^{-8} s^6 + 2.126 s^5 + \\ 180.8 s^4 + 1.464 \times 10^9 s^3 + 1.243 \times 10^{11} s^2 + \\ 2.376 \times 10^{15} s \end{pmatrix}}$$

(37)

Bode and root locus graphs can be sketched in Fig. 9 by using cascaded transfer function given in (37). It is observed by root locus that the maximum gain for stability of the controller is 0.0174. It can also be seen by root locus that there are six poles at $0.00262 \pm 3.82 \times 10^4$j, $-2.27 \times 10^{-13} \pm 3.6 \times 10^4$j, $-42.6 \pm 1.27 \times 10^3$j and two zeros at $4.07 \times 10^4 \pm 3.3 \times 10^4$j. By Bode plot, gain margin is -35.2 dB and phase margin is $-27.2°$, meaning that the open loop DC-DC isolated Ćuk converter with an LC filter is unstable as in the open loop transfer function of the converter.

The DC-DC isolated Ćuk converter is operated by using an LC input filter and the resulting waveforms are given in Fig. 10 showing the PWM signal, switch voltage, input current, and output voltage.
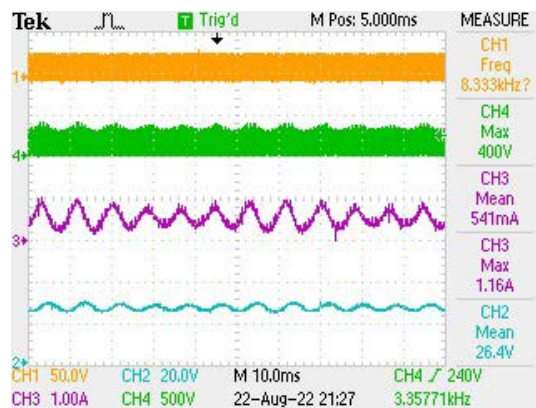
FIGURE 10. With LC filter, PWM signal, switch voltage, input current, output voltage.

The PWM signal, switch voltage, input current, and output voltage are given in Fig. 11 as a close-up of Fig. 10.

Fig. 12 shows the PWM signal, input voltage-current, and output voltage.

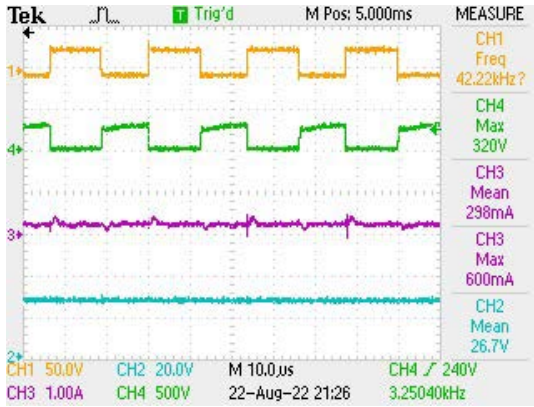Fig. 13 shows the PWM signal, input voltage, output current, and output voltage.

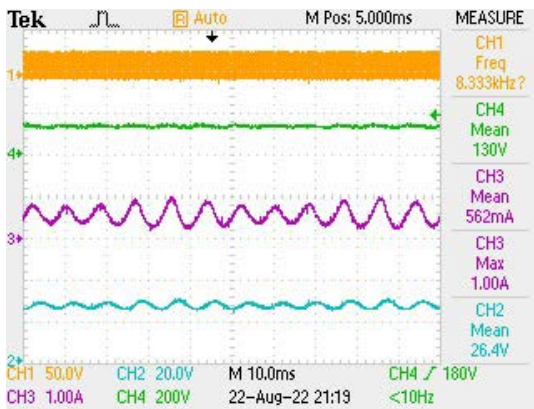**FIGURE 11.** With LC filter, PWM signal, switch voltage, input current, output voltage, zoomed.

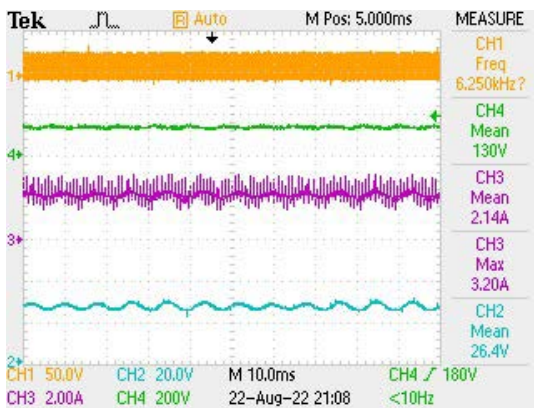**FIGURE 12.** With LC filter, PWM signal, input voltage-current, output voltage.

FIGURE 13. With LC filter, PWM signal, input voltage, output current, output voltage.

B. LCL FILTER WITH DAMPING

After cascading the transfer function of the LCL filter with damping given in (30) by using the passive value in Table 2, with the transfer function of the isolated Ćuk DC-DC converter in (36), the cascaded transfer function

is obtained in (38).

$$T(s) = \frac{\widetilde{V}_o}{\widetilde{d}} = \frac{\begin{pmatrix} 2.972s^4 + 6.294 \times 10^5 s^3 - \\ 6.284 \times 10^{10} s^2 + 2.402 \times 10^{15} s \end{pmatrix}}{\begin{pmatrix} 4.36 \times 10^{-22} s^9 + 1.4 \times 10^{-17} s^8 \\ + 6.8 \times 10^{-12} s^7 + 5.552 \times 10^{-8} s^6 \\ + 0.019 s^5 + 51.5 s^4 + 1.464 \times 10^7 s^3 + 1.324 \\ \times 10^9 s^2 + 2.4 \times 10^{13} s \end{pmatrix}}$$

(38)

Bode and root locus graphs can be sketched as in Fig. 14 by using the cascaded transfer function given in (38). It is observed by root locus that the maximum gain for stability of the controller is 0.0855. It can be seen by root locus that there are eight poles at $-1.55 \times 10^4 \pm 1.094 \times 10^5$j, $-8.11 \times 10^2 \pm 4.33 \times 10^4$j, $2.62 \times 10^{-3} \pm 3.82 \times 10^4$j, $-42.5 \pm 1.27 \times 10^3$j and three zeros at -2.93×10^5, $4.07 \times 10^4 \pm 3.3 \times 10^4$j. By Bode plot, gain margin is -21.4 dB and phase margin is $-26.2°$, meaning that the open loop DC-DC isolated Ćuk converter with an LCL filter with damping is unstable as in the open loop transfer function of the converter.
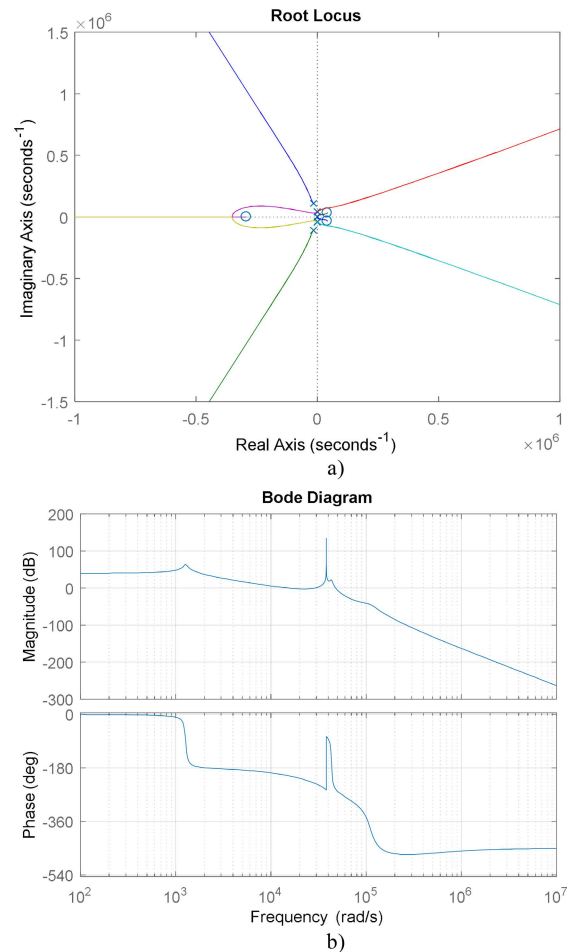

FIGURE 14. a) Root locus, b) Bode graphs of LCL filter with damping.

The DC-DC isolated Ćuk converter is operated by using an LCL with damping input filter and the resulting waveforms

are given in Fig. 15, showing the PWM signal, switch voltage, input current, and output voltage.

The PWM signal, switch voltage, input current, and output voltage are given in Fig. 16 as a close-up of Fig. 15.
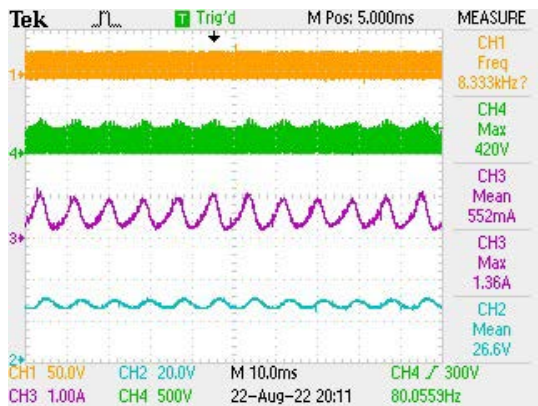

FIGURE 15. LCL filter with damping; PWM signal, switch voltage, input current, output voltage.
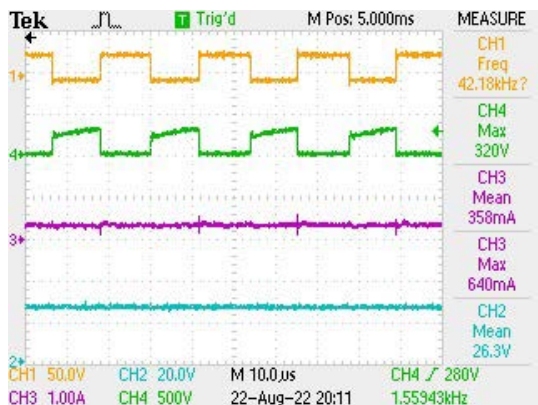

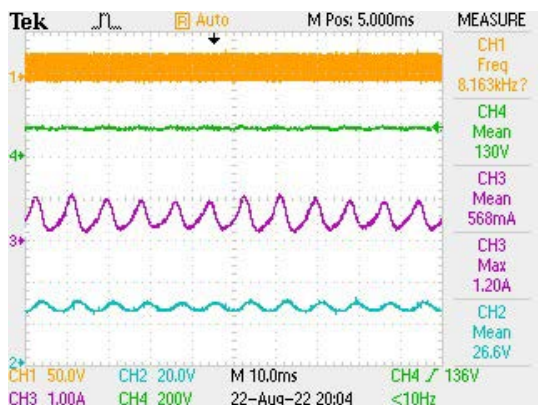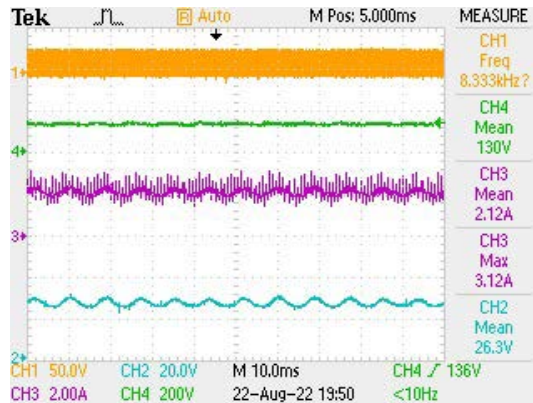**FIGURE 16.** LCL filter with damping; PWM signal, switch voltage, input current, output voltage, zoomed.

FIGURE 17. LCL filter with damping; PWM signal, input voltage-current, output voltage.

Fig. 17 shows the PWM signal, input voltage-current, and output voltage.

FIGURE 18. LCL filter with damping; PWM signal, input voltage, output current, output voltage.

Fig. 18 shows the PWM signal, input voltage, output current, and output voltage.

C. LCL FILTER

After cascading the transfer function of the LCL filter given in (31) by using the passive value in Table 2, with the transfer function of the isolated Ćuk DC-DC converter in (36) the cascaded transfer function is obtained in (39).

$$T(s) = \frac{\widetilde{V_o}}{\widetilde{d}} = \frac{871600s^3 - 7.103 \times 10^{10}s^2 + 2.4 \times 10^{15}s}{\begin{pmatrix} 4.36 \times 10^{-22}s^9 + 3.7 \times 10^{-20}s^8 \\ +4.8 \times 10^{-12}s^7 + 4.1 \times 10^{-10}s^6 + 0.016s^5 \\ +1.37s^4 + 1.46 \times 10^7s^3 + 1.243 \\ \times 10^9 s^2 + 2.376 \times 10^{13}s \end{pmatrix}}$$

(39)

Bode and root locus graphs can be sketched as in Fig. 19 by using the cascaded transfer function given in (39). It is observed by root locus that the maximum gain for stability of the controller is 0.0175. It can be seen by root locus that there are eight poles at $9.9 \times 10^{-8} \pm 7.1 \times 10^4$j, $-9.9 \times 10^{-8} \pm 6.74 \times 10^4$j, $2.62 \times 10^{-3} \pm 3.82 \times 10^4$j, $-42.5 \pm 1.27 \times 10^3$j and two zeros at $4.07 \times 10^4 \pm 3.3 \times 10^4$j. By Bode plot, gain margin is -35.2 dB and phase margin is $-25°$, meaning that the open loop isolated Ćuk converter with an LCL filter is unstable as in the open loop transfer function of the converter.

The DC-DC isolated Ćuk converter is operated by using an LCL input filter and the resulting waveforms are given in Fig. 20, showing the PWM signal, switch voltage, input current, and output voltage.

The PWM signal, switch voltage, input current, and output voltage are given in Fig. 21 as a close-up of Fig. 20.

Fig. 22 shows the PWM signal, input voltage-current, and output voltage.

Fig. 23 shows the PWM signal, input voltage, output current, and output voltage.

D. LCL TRAP FILTER

After cascading the transfer function of the LCL trap filter given in (35) by using the passive value in Table 2, with the
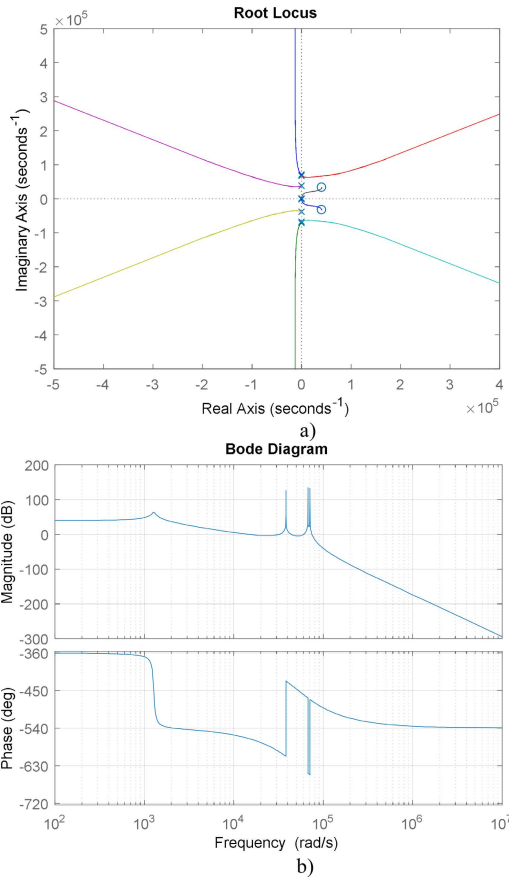
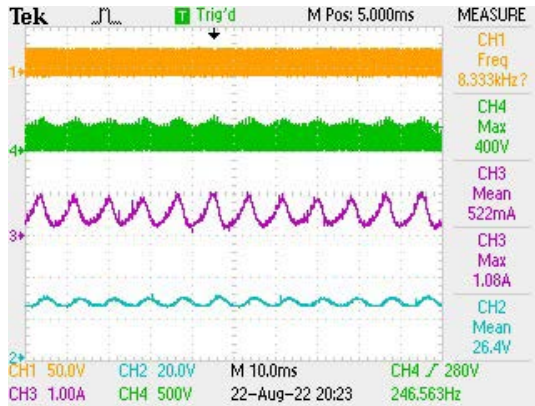**FIGURE 19.** a) Root locus, b) Bode graphs of LCL filter.

FIGURE 20. LCL filter; PWM signal, switch voltage, input current, output voltage.
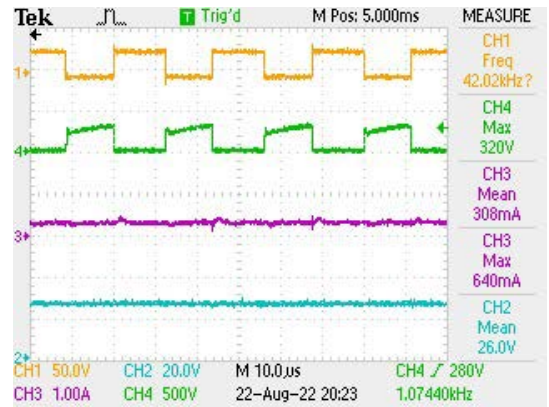

FIGURE 21. LCL filter; PWM signal, switch voltage, input current, output voltage, zoomed.
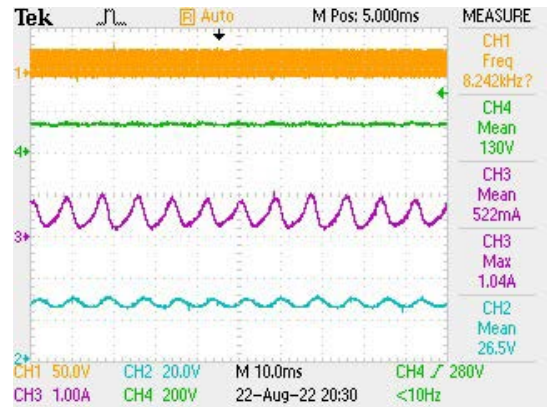

FIGURE 22. LCL filter; PWM signal, input voltage-current, output voltage.
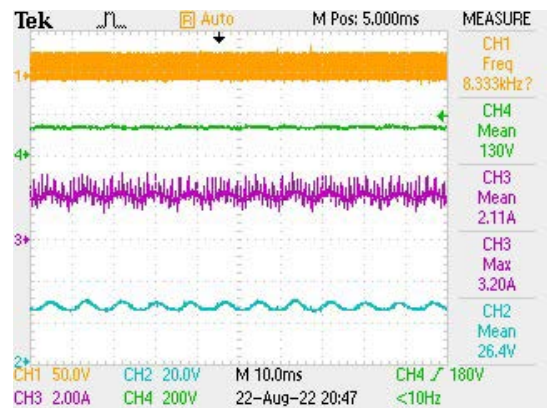

FIGURE 23. LCL filter; PWM signal, input voltage, output current, output voltage.

transfer function of the isolated Ćuk DC-DC converter in (36) the cascaded transfer function is obtained in (40).

$$T(s) = \frac{\widetilde{V_o}}{\widetilde{d}} = \frac{\begin{pmatrix} 1.25 \times 10^{-5}s^5 - 1.09s^4 + 9.061 \\ \times 10^5 s^3 - 7.103 \times 10^{10}s^2 + 2.402 \times 10^{15}s \end{pmatrix}}{\begin{pmatrix} 4.7 \times 10^{-22}s^9 + 3.97 \times 10^{-20}s^8 \\ + 6.8 \times 10^{-12}s^7 + 5.8 \times 10^{-10}s^6 + 0.019s^5 \\ + 1.62s^4 + 1.463 \times 10^7 s^3 + 1.243 \\ \times 10^9 s^2 + 2.37 \times 10^{13}s \end{pmatrix}}$$

(40)

Bode and root locus graphs can be sketched as in Fig. 24 by using the cascaded transfer function given in (40). It is observed by root locus that the maximum gain for stability of the controller is 0.0174. It can be seen by root locus that there are eight poles at $4.9 \times 10^{-14} \pm 1.06 \times 10^5$j, $-1.84 \times 10^{-13} \pm 4.35 \times 10^4$j, $2.62 \times 10^{-3} \pm 3.82 \times 10^4$j, $-42.5 \pm 1.27 \times 10^3$j and four zeros at $4.07 \times 10^4 \pm 3.3 \times 10^4$j,

$-3.36 \times 10^{-11} \pm 2.64 \times 10^5 \text{j}$. By Bode plot, gain margin is -35.2 dB and phase margin is $-26°$, meaning that the open loop isolated Ćuk converter with an LCL trap filter is unstable as in the open loop transfer function of the converter.
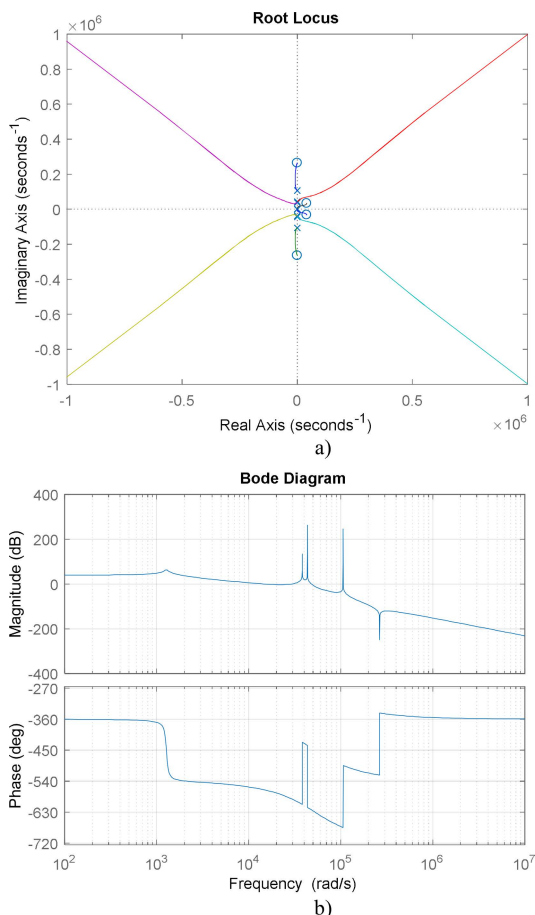

FIGURE 24. a) Root locus, b) Bode graphs of LCL trap filter.

The DC-DC isolated Ćuk converter is operated by using an LCL input filter and the resulting waveforms are given in Fig. 25, showing the PWM signal, switch voltage, input current, and output voltage.

The PWM signal, switch voltage, input current, and output voltage are given in Fig. 26 as a close-up of Fig. 25.

Fig. 27 shows the PWM signal, input voltage, input current, and output voltage.

Fig. 28 shows the PWM signal, input voltage, output current, and output voltage.

To provide the validity of the model and cascaded transfer function of the filters, step responses of each transfer function are sketched as in Fig. 29 under reference change. It is concluded from the figure that each cascaded transfer function of the filter and model of the converter is verified. However, the step response of the cascaded transfer function of the LCL with a damped converter has higher ripple values than the others. Each cascaded filter transfer function has similar results, although the converter gives 3 V lower at d equals '0.3' and 6 V lower at d equals '0.6' for step response.
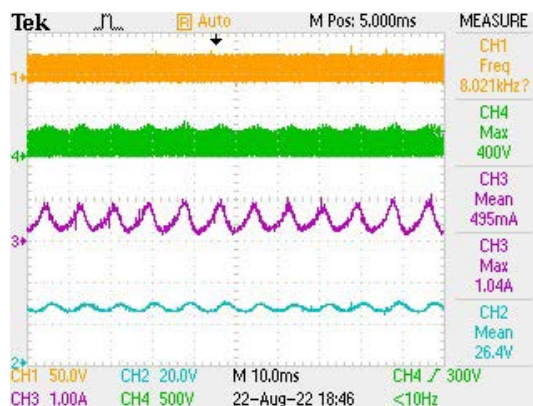

FIGURE 25. LCL trap filter; PWM signal, switch voltage, input current, output voltage.
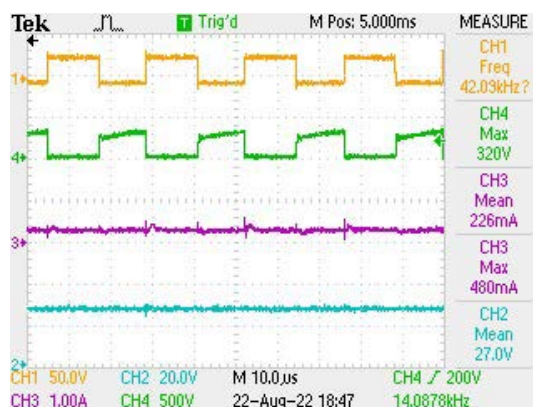

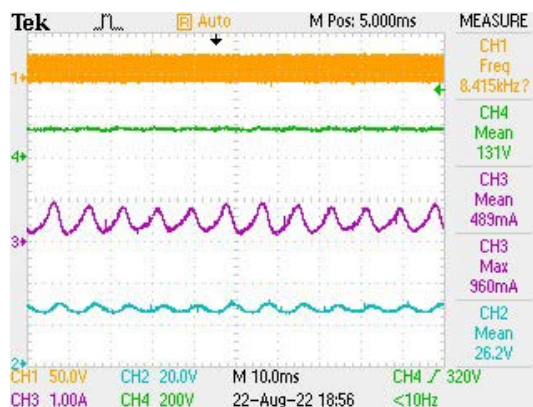FIGURE 26. LCL trap filter; PWM signal, switch voltage, input current, output voltage, zoomed.

FIGURE 27. LCL trap filter; PWM signal, input voltage-current, output voltage.

Comparison of the applications with respect to efficiency at full load and input current maximum ripple is given by each filter in Table 3. It can be concluded from Table 3 that the LCL trap filter is better than other filter structures in terms of efficiency and current ripple. Furthermore, the maximum allowable gain of the controller for stability is 0.0174, 0.0855, 0.0175, and 0.0174 for LC, LCL with damping, LCL, and LCL trap, respectively.
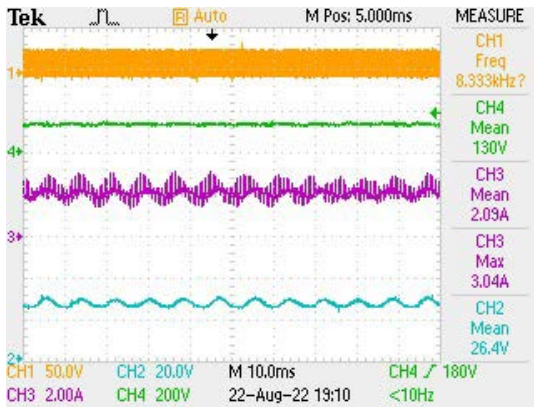
FIGURE 28. LCL trap filter; PWM signal, input voltage, output current, output voltage.
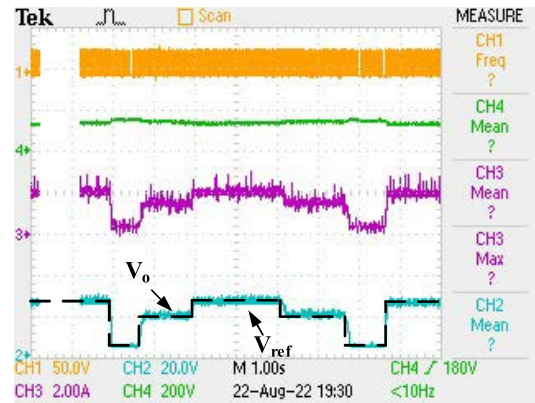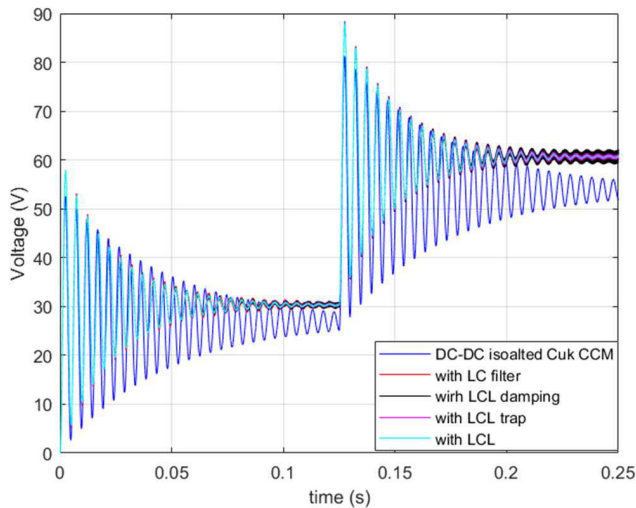

FIGURE 29. Step responses of each cascaded transfer function and isolated DC-DC Cuk converter.

TABLE 3. Comparison of filters.

LC		LCL damp.		with LCL		LCL trap	
Eff.	Cur. Peak (A)	Eff.	Cur. Peak (A)	Eff.	Cur. Peak (A)	Eff.	Cur. Peak (A)
77%	1	75.5%	1.2	82%	1.04	86%	0.96

Fig. 30 shows the PWM signal, input voltage, output current, and output voltage. In the figure output voltage is controlled by the PI controller under reference changes. By means of the controller, output voltage is regulated as desired by the reference voltage. Each filter has similar closed loop control characteristics.

V. DISCUSSIONS

This paper presents the application, analysis, and comparison of an LCL type filter with a DC-DC isolated Cuk converter operated in CCM by using a SiC power switch. Moreover, the

FIGURE 30. Output voltage of the converter under reference changes.

paper presents a state-space average model, small signal analysis, and transfer function of a DC-DC isolated Cuk converter for CCM operation, which was not included in the literature before. As a result, it is shown that compared to other filter types, the LCL trap filter, which is not presented for a DC-DC converter in the literature, provides better efficiency (86%) and lower input current ripple (0.96 A). In addition, regarding the control characteristics, the LCL with damping filter gives poorer results because of higher voltage ripple, as shown in the step response in Fig. 29, of open loop cascaded transfer functions, despite having higher allowable gain, that is 0.0855, for stability. However, the closed loop response with a PI controller under reference changes given in Fig. 30 is similar for each filter structure.

In the literature, such comparison, analysis, and application of the filter types considering converter transfer function especially by using an LCL trap filter for the isolated Cuk DC-DC converter are not presented. However, comparisons of the L, LC, and LCL filters in [37], [38], [41], and [42], and LC and LCL trap filters in [43] and [44] are given for three phase rectifiers and inverter with respect to total harmonic distortion and power factor without considering the effect of the transfer function of the converter. It is stated in [37], [38], [41], and [42] that the LCL filter has better attenuation compared to L and LC filters. Further, [43] and [44] state that the LCL trap filter has better attenuation than the LCL filter in rectifier or inverter studies. Similarly, in the present study the LCL trap filter gives better results for the isolated Cuk DC-DC converter. In addition, [37] and [40] state that by using an LCL filter the total inductor value is less than that of L and LC filters as it is presented in this paper that there is a 45% inductor reduction with respect to the LC filter. Although [48], [49], and [50] introduce the analysis of just LC filters considering the converter effect, they do not include the application and examination of input current ripple for DC-DC converters as given in this paper.

Furthermore, as a limitation of the study, the open loop cascaded transfer function of both the filter and DC-DC isolated Cuk converter have unstable Bode plots. This is the same as the open loop Bode plots of the transfer functions of Cuk, boost, and SEPIC converters given in [60], [61], [62],

and [63]. Such unstable Bode plots are usual for power converters having nonminimum phase transfer functions.

Another issue as a limitation in the paper is higher filter inductor values. Nonetheless, as given in the design equations (24), (33) choosing different capacitor values can ensure lower inductor values of the filter.

Moreover, the accuracy of the converter transfer function and the cascaded transfer functions presented in the paper is validated by step responses.

VI. CONCLUSION

Herein, the application of LCL type input filter topologies including LCL, LCL with damping, and LCL trap filters with a DC-DC isolated Ćuk converter designed for 50 W power with 42 kHz switching frequency at CCM operation by using a SiC power switch is realized. In the literature, LCL type filters are not presented in detail with a DC-DC converter. Therefore, one of the main unique contributions of the paper is the design, analyses, and implementation of an LCL trap filter, which is not presented in the literature for a DC-DC converter, as an input filter of a DC-DC isolated Ćuk converter. By means of the applications, a comparison is made with respect to efficiency, input current ripple, and control point of view. Moreover, to make a general comparison a LC type filter is included. As a second unique contribution of the paper, a state-space average model of the DC-DC isolated Ćuk converter operated in CCM is derived, small signal analysis is conducted, and a transfer function is obtained, and the transfer function is analyzed by linear methods including root locus and Bode graphs. In addition, the transfer function and practical design of each filter topology are presented and cascaded transfer functions with the DC-DC isolated Ćuk converter are derived. Furthermore, verification of the modeling of the converter and each cascaded transfer function is performed by step responses. Then the effects of each filter topology on the transfer functions are analyzed by linear methods for the control point of view as such analysis has not been introduced in the literature before. Due to the applications, the effects of each filter on efficiency and input current ripple are compared. As a result, the LCL trap filter is better than the others by giving 86% efficiency and 0.96 A input current ripple. Moreover, the total inductor value with the LCL filter is reduced 45% compared to the LC filter. Further, for the control point of view, each filter has similar closed loop characteristics. Although the maximum gain of the controller avoiding instability of LCL with damping is 0.0855, which is higher than that of the others, LCL with damping has poorer control response.

By using a multi-tuned filter structure in future work, it is assumed that better input current ripple reduction can be obtained.

REFERENCES

[1] R. N. Beres, X. Wang, M. Liserre, F. Blaabjerg, and C. L. Bak, "A review of passive power filters for three-phase grid-connected voltage-source converters," *IEEE Trans. J. Emerg. Sel. Topics Power Electron.*, vol. 4, no. 1, pp. 54–69, Mar. 2016, doi: 10.1109/JESTPE.2015.2507203.

[2] A. Reznik, M. G. Simoes, A. Al-Durra, and S. M. Muyeen, "*LCL* filter design and performance analysis for grid-interconnected systems," *IEEE Trans. Ind. Appl.*, vol. 50, no. 2, pp. 1225–1232, Jul. 2013, doi: 10.1109/TIA.2013.2274612.

[3] D. Rothmund, T. Guillod, D. Bortis, and J. W. Kolar, "99.1% efficient 10 kV SiC-based medium-voltage ZVS bidirectional single-phase PFC AC/DC stage," *IEEE J. Emerg. Sel. Topics Power Electron.*, vol. 7, no. 2, pp. 779–797, Jun. 2019, doi: 10.1109/JESTPE.2018.2886140.

[4] R. Kushwaha and B. Singh, "UPF-isolated zeta converter-based battery charger for electric vehicle," *IET Electr. Syst. Transp.*, vol. 9, no. 3, pp. 103–112, May 2019, doi: 10.1049/iet-est.2018.5010.

[5] R. N. Beres, X. Wang, F. Blaabjerg, M. Liserre, and C. L. Bak, "Optimal design of high-order passive-damped filters for grid-connected applications," *IEEE Trans. Power Electron.*, vol. 31, no. 4, pp. 2083–2098, Mar. 2016, doi: 10.1109/TPEL.2015.2441299.

[6] J. Fang, X. Li, X. Yang, and Y. Tang, "An integrated trap-LCL filter with reduced current harmonics for grid-connected converters under weak grid conditions," *IEEE Trans. Power Electron.*, vol. 32, no. 11, pp. 8446–8457, Nov. 2017, doi: 10.1109/TPEL.2017.2651152.

[7] F. Li, X. Zhang, H. Zhu, H. Li, and C. Yu, "An LCL-LC filter for grid-connected converter: Topology, parameter, and analysis," *IEEE Trans. Power Electron.*, vol. 30, no. 9, pp. 5067–5077, Sep. 2015, doi: 10.1109/TPEL.2014.2367135.

[8] M. Azab, "Design approach and performance analysis of trap filter for three-phase PV grid integration systems using evolutionary search algorithms," *J. King Saud Univ. Eng. Sci.*, vol. 33, no. 7, pp. 491–506, Nov. 2021, doi: 10.1016/j.jksues.2020.06.002.

[9] S. Piasecki, A. M. Canterallas, J. Rabkowski, and P. Rodriguez, "Design of AC-DC power converters with LCL + tuned trap line filter using Si IGBT and SiC MOSFET modules," in *Proc. 39th Annu. Conf. IEEE Ind. Electron. Soc. (IECON)*, Vienna, Austria, Nov. 2013, pp. 5957–5962.

[10] M. S. Makowski and A. J. Forsyth, "Modeling and analysis of the fully-integrated magnetics DC-isolated Cuk converter," in *Proc. 5th Eur. Conf. Power Electron. Appl.*, Brighton, U.K., pp. 202–207, Sep. 1993.

[11] L. D. Stevanovic and S. Cuk, "Input current shaping and regulation of multiple outputs in a single isolated converter," in *Proc. Intelec 93, 15th Int. Telecommun. Energy Conf.*, Paris, France, 1993, pp. 326–333.

[12] R. D. Middlebrook and S. Cuk, "Isolation and multiple output extensions of a new optimum topology switching DC-to-DC converter," in *Proc. IEEE Power Electron. Specialists Conf.*, Syracuse, NY, USA, Jun. 1978, pp. 256–264.

[13] V. Vorperian, "The effect of the magnetizing inductance on the small-signal dynamics of the isolated Cuk converter," *IEEE Trans. Aerosp. Electron. Syst.*, vol. 32, no. 3, pp. 967–983, Jul. 1996, doi: 10.1109/7.532257.

[14] S. Gangavarapu, A. K. Rathore, and D. M. Fulwani, "Three-phase single-stage-isolated Cuk-based PFC converter," *IEEE Trans. Power Electron.*, vol. 34, no. 2, pp. 1798–1808, Feb. 2019, doi: 10.1109/TPEL.2018.2829080.

[15] S. Pal, B. Singh, A. Shrivastava, A. Chandra, and K. Al-Haddad, "Improved power quality opto-coupler less Cuk converter for flicker less LED lighting," in *Proc. IEEE Energy Conversion Congr. Expo. (ECCE)*, Montreal, QC, Canada, Sep. 2015, pp. 3239–3246.

[16] J. R. Nolasco, G. M. Soarez, and H. A. C. Braga, "High power factor converter for LED drivers based on isolated Ćuk topology," in *Proc. Simposio Brasileiro de Sistemas Eletricos (SBSE)*, Niteroi, Brazil, May 2018, pp. 1–6.

[17] V. Bist and B. Singh, "A unity power factor bridgeless isolated Cuk converter fed brushless DC motor drive," *IEEE Trans. Ind. Electron.*, vol. 62, no. 7, pp. 4118–4129, Jul. 2015, doi: 10.1109/TIE.2014.2384001.

[18] A. Anand, B. Singh, A. Chandra, and K. Al-Haddad, "Isolated Cuk converter with two symmetrical output voltages for SRM drive," in *Proc. IEEE Wireless Power Transf. Conf. (WPTC)*, Montreal, QC, Canada, Jun. 2018, pp. 1–4.

[19] R. Kushwaha and B. Singh, "A unity power factor converter with isolation for electric vehicle battery charger," in *Proc. IEEMA Engineer Infinite Conf. (eTechNxT)*, New Delhi, India, Mar. 2018, pp. 1–6.

[20] G. Kumar and B. Singh, "Dual-input single-stage isolated charger for light electric vehicles," in *Proc. IEEE Int. Power Renew. Energy Conf. (IPRECON)*, Kollam, India, Sep. 2021, pp. 1–6.

[21] A. Nadler, "Impact of the layout, components, and filters on the EMC of modern DC/DC switching controllers," Würth Elektronik, Waldenburg, Germany, Tech. Rep. ANP044, 2017.

[22] M. Sclocchi, "Input filter design for switching power supplies," Texas Instruments, Dallas, TX, USA, Tech. Rep. SNVA538, 2010.

[23] V. Dzhankhotov and J. Pyrhonen, "Passive LC filter design considerations for motor applications," *IEEE Trans. Ind. Electron.*, vol. 60, no. 10, pp. 4253–4259, Oct. 2013, doi: 10.1109/TIE.2012.2209612.

[24] Q. He, L. Liu, M. Qiu, and Q. Luou, "A step-by-step design for low-pass input filter of the single-stage converter," *Energies*, vol. 14, no. 23, pp. 1–25, Nov. 2021, doi: 10.3390/en14237901.

[25] J. M. Sosa, G. Escobar, P. R. M. Rodriguez, G. Vazquez, M. A. Juarez, and J. C. N. Cruz, "A model-based controller for a DC–DC boost converter with an LCL input filter," in *Proc. 41st Annu. Conf. IEEE Ind. Electron. Society (IECON)*, Yokohama, Japan, Nov. 2015, pp. 000619–000624.

[26] C. A. Felipe, E. L. Carvalho, E. G. Carati, L. Michels, L. V. Bellinaso, and R. Cardoso, "Analytical methodology to design third-order filter (LCL) for battery chargers," in *Proc. IEEE Int. Conf. Ind. Technol. (ICIT)*, Buenos Aires, Argentina, Feb. 2020, pp. 444–449.

[27] Y. Deng, J. Liu, W. Tang, X. Wei, X. Han, and C. Feng, "Stability analysis of bi-directional DC–DC converter based on battery energy storage," in *Proc. Int. Conf. Intell. Comput., Autom. Syst. (ICICAS)*, Chongqing, China, Dec. 2021, pp. 84–89.

[28] M. B. S. Romdhane, M. W. Naouar, I. S. Belkhodja, and E. Monmasson, "An Improved LCL filter design in order to ensure stability without damping and despite large grid impedance variations," *Energies*, vol. 10, no. 3, pp. 1–19, Mar. 2017, doi: 10.3390/en10030336.

[29] H. A. Young, V. A. Marin, C. Pesce, and J. Rodriguez, "Simple finite-control-set model predictive control of grid-forming inverters with LCL filters," *IEEE Access*, vol. 8, pp. 81246–81256, 2020, doi: 10.1109/ACCESS.2020.2991396.

[30] V. Miskovic, V. Blasko, T. M. Jahns, A. H. C. Smith, and C. Romenesko, "Observer-based active damping of LCL resonance in grid-connected voltage source converters," *IEEE Trans. Ind. Appl.*, vol. 50, no. 6, pp. 3977–3985, Apr. 2014, doi: 10.1109/TIA.2014.2317849.

[31] H. Zhao, Y. Shen, W. Ying, S. S. Ghosh, M. R. Ahmed, and T. Long, "A single- and three-phase grid compatible converter for electric vehicle on-board chargers," *IEEE Trans. Power Electron.*, vol. 35, no. 7, pp. 7545–7562, Jul. 2020, doi: 10.1109/TPEL.2019.2956653.

[32] E. Sanal and P. Dost, "LCL filter design for a battery charger based on buck converter (DCDC converter)," in *Proc. IEEE Int. Conf. Renew. Energy Res. Appl. (ICRERA)*, Birmingham, U.K., Nov. 2016, pp. 617–621.

[33] O. Atmaca, E. Erol, T. Kamal, and M. Karabacak, "Design of an H-bridge bidirectional DC–DC converter with LCL filter for high power battery applications," in *Proc. 1st Global Power, Energy Commun. Conf. (GPECOM)*, Nevsehir, Turkey, Jun. 2019, pp. 238–241.

[34] S. Jayalath and M. Hanif, "Generalized LCL-filter design algorithm for grid-connected voltage-source inverter," *IEEE Trans. Ind. Electron.*, vol. 64, no. 3, pp. 1905–1915, Mar. 2017, doi: 10.1109/TIE.2016.2619660.

[35] A. Kouchaki and M. Nymand, "Analytical design of passive LCL filter for three-phase two-level power factor correction rectifiers," *IEEE Trans. Power Electron.*, vol. 33, no. 4, pp. 3012–3022, Apr. 2018, doi: 10.1109/TPEL.2017.2705288.

[36] Y. Patel, D. Pixler, and A. Nasiri, "Analysis and design of TRAP and LCL filters for active switching converters," in *Proc. IEEE Int. Symp. Ind. Electron.*, Niteroi, Brazil, Jul. 2010, pp. 638–643.

[37] U. P. Yagnik and M. D. Solanki, "Comparison of L, LC & LCL filter for grid connected converter," in *Proc. Int. Conf. Trends Electron. Informat. (ICEI)*, Tirunelveli, India, May 2017, pp. 455–458.

[38] R. Kong, L. K. Kuan, and M. Z. B. Daud, "Comparison of efficiency of double conversion UPS with LC, LCL and LCL with damping resistor filters," in *Proc. IEEE Conf. Energy Convers. (CENCON)*, Johor Bahru, Malaysia, Oct. 2021, pp. 34–39.

[39] J. D. Vidal, O. Carranza, J. J. Rodriguez, L. G. Gonzalez, and R. Ortega, "Analysis of the response of L and LCL filters in controlled rectifiers used in wind generator systems with permanent magnet synchronous generators," *IEEE Latin Amer. Trans.*, vol. 16, no. 8, pp. 2145–2152, Aug. 2018, doi: 10.1109/TLA.2018.8528228.

[40] G. Ye, M. Babar, and J. F. G. Cobben, "Performance comparison of different filter applications in three-phase PFC rectifier," presented at the 2014 14th Int. Conf. Environment and Electrical Engineering, Krakow, Poland, May 2014, pp. 437–442.

[41] J. M. Sosa, G. Escobar, P. R. Martinez-Rodriguez, G. Vazquez, M. A. Juarez, and M. Diosdado, "Comparative evaluation of L and LCL filters in transformerless grid tied converters for active power injection," in *Proc. IEEE Int. Autumn Meeting Power, Electron. Comput. (ROPEC)*, Ixtapa, Mexico, Nov. 2014, pp. 1–6.

[42] A. Dolara, G. Magistrati, R. Zich, L. Frosio, and G. Marchegiani, "Harmonic analysis of output filters for grid connected converters in battery energy storage systems," in *Proc. 16th Int. Conf. Harmon. Quality Power (ICHQP)*, Bucharest, Romania, May 2014, pp. 162–166.

[43] S. Piasecki and M. P. Kazmierkowski, "Advanced grid filters for AC-DC converters—Analysis and design methodology," in *Proc. 13th Select. Issues Elect. Eng. Electron. (WZEE)*, Rzeszow, Poland, May 2016, pp. 1–5.

[44] R. Chakroun, R. B. Ayed, and N. Derbel, "Comparison between LCL and LLCL filters for a grid connected inverter using selective harmonic modulation," in *Proc. 5th Int. Conf. Renew. Energies Developing Countries (REDEC)*, Marrakech, Morocco, Jun. 2020, pp. 1–6.

[45] L. Zhai, G. Hu, M. Lv, T. Zhang, and R. Hou, "Comparison of two design methods of EMI filter for high voltage power supply in DC–DC converter of electric vehicle," *IEEE Access*, vol. 8, pp. 66564–66577, 2020, doi: 10.1109/ACCESS.2020.2985528.

[46] L. Zhai, G. Hu, C. Song, M. Lv, and X. Zhang, "Comparison of two filter design methods for conducted EMI suppression of PMSM drive system for electric vehicle," *IEEE Trans. Veh. Technol.*, vol. 70, no. 7, pp. 6472–6484, Jul. 2021, doi: 10.1109/TVT.2021.3080924.

[47] S. Jiang, Y. Liu, Z. Mei, J. Peng, and C.-M. Lai, "A magnetic integrated LCL–EMI filter for a single-phase SiC-MOSFET grid-connected inverter," *IEEE J. Emerg. Sel. Topics Power Electron.*, vol. 8, no. 1, pp. 601–617, Mar. 2020, doi: 10.1109/JESTPE.2019.2937816.

[48] M. U. Iftikhar, A. Bilal, D. Sadarnac, P. Lefranc, and C. Karimi, "Analysis of input filter interactions in cascade buck converters," in *Proc. IEEE Int. Conf. Ind. Technol.*, Chengdu, China, Apr. 2008, pp. 1–6.

[49] M. U. Iftikhar, D. Sadarnac, and C. Karimi, "Conducted EMI suppression and stability issues in switch-mode DC–DC converters," in *Proc. IEEE Int. Multitopic Conf.*, Islamabad, Pakistan, Dec. 2006, pp. 389–394.

[50] Y. Huangfu, S. Pang, B. Nahid-Mobarakeh, L. Guo, A. K. Rathore, and F. Gao, "Stability analysis and active stabilization of on-board DC power converter system with input filter," *IEEE Trans. Ind. Electron.*, vol. 65, no. 1, pp. 790–799, Jan. 2018, doi: 10.1109/TIE.2017.2703663.

[51] Z. Lin, Y. Liu, X. He, W. Xie, M. Dong, and F. Wang, "Closed-loop stability analysis of DC/DC converter with input filter," in *Proc. IEEE Int. Conf. Inf. Technology, Big Data Artif. Intell. (ICIBA)*, Chongqing, China, Nov. 2020, pp. 397–403.

[52] X. Yu and M. Salato, "An optimal minimum-component DC–DC converter input filter design and its stability analysis," *IEEE Trans. Power Electron.*, vol. 29, no. 2, pp. 829–840, Feb. 2014, doi: 10.1109/TPEL.2013.2257860.

[53] M. Wu, D. D.-C. Lu, and C. K. Tse, "Direct and optimal linear active methods for stabilization of LC input filters and DC/DC converters under voltage mode control," *IEEE J. Emerg. Sel. Topics Circuits Syst.*, vol. 5, no. 3, pp. 402–412, Sep. 2015, doi: 10.1109/JETCAS.2015.2462171.

[54] R. Roy and S. Kapat, "Input filter-based ripple injection for mitigating limit cycling in buck converters driving CPL," *IEEE J. Emerg. Sel. Topics Power Electron.*, vol. 9, no. 2, pp. 1315–1327, Apr. 2021, doi: 10.1109/JESTPE.2020.2985426.

[55] S. Pang, B. Nahid-Mobarakeh, S. Pierfederici, Y. Huangfu, G. Luo, and F. Gao, "Toward stabilization of constant power loads using IDA-PBC for cascaded LC filter DC/DC converters," *IEEE J. Emerg. Sel. Topics Power Electron.*, vol. 9, no. 2, pp. 1302–1314, Apr. 2021, doi: 10.1109/JESTPE.2019.2945331.

[56] R. Gavagsaz-Ghoachani, M. Phattanasak, J.-P. Martin, S. Pierfederici, B. Nahid-Mobarakeh, and P. Riedinger, "A Lyapunov function for switching command of a DC–DC power converter with an LC input filter," *IEEE Trans. Ind. Appl.*, vol. 53, no. 5, pp. 5041–5050, Sep. 2017, doi: 10.1109/TIA.2017.2715325.

[57] M. S. Chayjani and M. Monfared, "Stability analysis and robust design of LCL with multituned traps filter for grid-connected converters," *IEEE Trans. Ind. Electron.*, vol. 63, no. 11, pp. 6823–6834, Nov. 2016, doi: 10.1109/TIE.2016.2582792.

[58] F. M. M. Rahman, V. Pirsto, J. Kukkola, M. Routimo, and M. Hinkkanen, "State-space control for LCL filters: Converter versus grid current measurement," *IEEE Trans. Ind. Appl.*, vol. 56, no. 6, pp. 6608–6618, Nov. 2020, doi: 10.1109/TIA.2020.3016915.

[59] J. Dannehl, F. W. Fuchs, and P. B. Thøgersen, "PI state space current control of grid-connected PWM converters with LCL filters," *IEEE Trans. Power Electron.*, vol. 25, no. 9, pp. 2320–2330, Sep. 2010, doi: 10.1109/TPEL.2010.2047408.

[60] B. K. Kushwaha and A. Narain, "Controller design for Cuk converter using model order reduction," in *Proc. 2nd Int. Conf. Power, Control Embedded Syst.*, Allahabad, India, Dec. 2012, pp. 1–5.

[61] G. Abbas, U. Farooq, J. Gu, and M. U. Asad, "Controller design for low-input voltage switching converters having non-minimum phase characteristics," in *Proc. IEEE 28th Can. Conf. Electr. Comput. Eng. (CCECE)*, Halifax NS, Canada, May 2015, pp. 1294–1298.

[62] B. Chandan, P. Dwivedi, and S. Bose, "Closed loop control of SEPIC DC–DC converter using loop shaping control technique," in *Proc. IEEE 10th Control Syst. Graduate Res. Colloq. (ICSGRC)*, Shah Alam, Malaysia, Aug. 2019, pp. 20–25.

[63] S. Surya and S. Williamson, "Generalized circuit averaging technique for two-switch PWM DC–DC converters in CCM," *Electronics*, vol. 10, no. 4, pp. 1–15, Feb. 2021, doi: 10.3390/electronics10040392.

ERDAL ŞEHIRLI was born in Kastamonu, Turkey, in 1983. He received the first B.S. degree in electrical education from Gazi University, in 2006, the second B.S. degree in electrical engineering from Istanbul Technical University, in 2016, and the first M.S. degree in electrical education, the second M.S. degree in electrical engineering, and the Ph.D. degree in electricity education from Kocaeli University, Turkey, in 2009, 2016, and 2017, respectively.

From 2009 to 2018, he was a Lecturer at the Vocational College of Higher Education, Kastamonu University. Since 2018, he has been an Assistant Professor with the Department of Electrical Engineering, Kastamonu University. His research interests include power electronics and control systems and microgrids.

● ● ●